Summer 2017

The Role of Hemodynamic Force on Development of the Mouse Embryonic Heart

Samantha Jean Fredrickson
Missouri State University, Fredrickson221@live.missouristate.edu

THE ROLE OF HEMODYNAMIC FORCE ON DEVELOPMENT OF THE MOUSE EMBRYONIC HEART

A Masters Thesis

Presented to

The Graduate College of

Missouri State University

In Partial Fulfillment

Of the Requirements for the Degree

Master of Science, Biology

By

Samantha J. Fredrickson

August 2017

THE ROLE OF HEMODYNAMIC FORCE ON DEVELOPMENT OF THE MOUSE EMBRYONIC HEART

Biology

Missouri State University, August 2017

Master of Science

Samantha J. Fredrickson

ABSTRACT

The most common type of birth defects are congenital heart defects (or CHDs). Though a few cases of CHDs have been attributed to genetic defects specific to the heart, substance exposure, or to maternal disease, the cause of most CHDs is unknown. Thus, further research is needed to determine how CHDs form. Very few studies have investigated how physiological factors like perturbations of blood flow can affect normal heart development. For instance, increasing or decreasing the resistance to blood flow can alter development of the heart in both zebrafish and chicken embryos. This could be one mechanism to explain CHD formation, but further investigation in a mammalian system is needed. To examine this idea, I experimentally manipulated cultured mouse embryos, testing the effects of decreased blood viscosity (to create low hemodynamic force [cardiovascular system] or low hemodynamic loading [heart-specific]). To determine the effects on heart development, I prepared the embryos for 3D imaging by optical projection tomography (OPT), and assessed heart volume and myocardial thickness. There was no detectable change in the volume of hearts under low hemodynamic force compared to hearts with normal hemodynamic force. However, I did observe a decrease of myocardial thickness in hearts with low hemodynamic force compared to control hearts. Thus, this study demonstrates that even at very early stages of embryonic development, alterations in blood flow can influence heart development. This indicates CHD formation can be exacerbated upon initial exposure to a primary cause (genetic defects, substance exposure or maternal disease) due to changes in hemodynamic forces.

KEYWORDS: congenital heart defects, mouse embryo, heart development, hemodynamic force, hemodynamic loading, embryo culture

This abstract is approved as to form and content

_____

Ryan Udan, PhD.
Chairperson, Advisory Committee
Missouri State University

THE ROLE OF HEMODYNAMIC FORCE ON DEVELOPMENT OF THE MOUSE EMBRYONIC HEART

By

Samantha J. Fredrickson

A Masters Thesis
Submitted to the Graduate College
Of Missouri State University
In Partial Fulfillment of the Requirements
For the Degree of Master of Science

August 2017

Approved:

_____
Ryan Udan, PhD

_____
Paul Durham, PhD

_____
Christopher Lupfer, PhD

_____
Julie Masterson, PhD: Dean, Graduate College

ACKNOWLEDGEMENTS

I would like to thank Dr. Ryan Udan for his support during my graduate studies and efforts toward my development as a scientific professional. I am also grateful to my thesis committee members Dr. Paul Durham and Dr. Christopher Lupfer for their time and expertise perfecting this thesis. I would also like to thank my lab mates: Rachel Padget, Shilpa Mohite, and Tanner Hoog for their assistance with this research (especially Tanner for his help imaging and collecting data). A big thank you to Jim Church for his help with statistics. The project was made possible by funds I received from the Biology department and the Graduate College at MSU and thanks to the use of the OPT, courtesy of the Dickinson lab (Henry Le) and the Optical Imaging and Vital Microscopy Core (Logan Hsu and Tegy Vedakkan) at Baylor College of Medicine. I would like to also thank Sara Woodman and her family for taking me in to their home for two weeks after my apartment complex was set on fire twice while writing this thesis. Last but not least, thank you to my friends and family for their support.

TABLE OF CONTENTS

LIST OF TABLES

LIST OF FIGURES

INTRODUCTION

The Cardiovascular System

The cardiovascular system is comprised of the heart and blood vessels that function to pump and distribute blood (for oxygenation) and plasma (containing nutrients, waste products, and other molecules) throughout the rest of the body. At the core of the cardiovascular system is the heart. In mammals, the heart is a four-chambered structure, composed of right and left atria, which pump blood into ventricles, and the right and left ventricles, which pump blood into the lungs and rest of the body. Blood exits the heart and into the rest of the body via the circulatory system which is comprised of an interconnected, branched system of arteries that feed into tiny capillaries, and finally these become collected back into veins that bring blood back to the heart (Udan et al., 2013).

The heart is a very critical structure for survival of vertebrate organisms because without its function, the organism would be deprived of oxygen and nutrients (Buckingham et al., 2005). Proper functioning of the adult heart relies upon a coordination of contraction between atria and ventricles, the proper presence of septa, and valves, all of which allow for the forward movement of blood (van Weerd and Christoffels, 2016).

There are many ways in which the heart can fail to function (heart failure or HF). The most common cause of defective heart function is a myocardial infarction (MI, commonly known as a heart attack). MIs occur when blood flow to the heart via the coronary arteries is cut off (Keeley et al., 2003). This results in death of the myocardium

and can be lethal (Daubert and Jeremias, 2010). Though myocardial infarction is a product of atherosclerosis (vascular disease), this usually occurs in adulthood due to a complex mixture of environmental and other risk factors. Defective heart function does not exclusively occur in adulthood. Many functional issues are caused by defects resulting from improper development of the heart that occurs during embryogenesis and fetal development.

Congenital Heart Defects

Birth defects impacting the morphology and function of the heart are the most common and lethal type of birth defects (Jenkins et al., 2007). These defects are called congenital heart defects (CHDs). Some CHDs go unnoticed or have such minimal effects on the organ's function that treatment is not needed, whereas others require treatment soon after birth (Bull, 1999).

Though CHDs occur in about 1 out of 100 births, the ratio would be higher if it included embryos with CHDs (Hoffman, 1995). This can be explained by the fact that defects in embryonic heart development can result in spontaneous abortions (miscarriages), particularly in the first trimester, and thus they would never be reported as having a CHD (Bruneau, 2008; Goldstein, 1994; Makikallio et al., 2005).

There are many known causes for CHDs. These causes can be categorized into three groups: maternal disease, substance exposures, and genetic causes. First, maternal health is crucial for the proper development of offspring. Unfortunately, there are many diseases and conditions a mother can have that may negatively impact a developing embryo. One study on women with phenylketonuria found those who do not regulate

their diet have >12% chance of having a child born with a CHD (Rouse and Azen, 2004). Mothers with unmanaged diabetes have 3-5 times the risk of having offspring with a CHD (Nassr et al., 2016) than healthy mothers. Maternal epilepsy is associated with CHDs. However, it has been difficult to parse apart the effects of the condition versus the effects of treatments for epilepsy. Many of the treatments for epilepsy disrupt the metabolism of folate, a necessary component of the maternal diet. Lastly, infections during pregnancy such as Influenza (and many other disease accompanied by a persistent fever) are also associated with an increased risk of CHDs (Jenkins et al., 2007; Oster et al., 2011).

Another way CHDs have been induced is through exposure of the mother to teratogenic substances and/or lack of nutrients needed in her diet. Teratogens, such as thalidomide, are known to cause congenital deformities including phocomelia (limb deformities (Vargesson, 2009)) and of course, CHDs (Smithells and Newman, 1992). Some studies have found an association between cigarette smoking and CHDs, but these findings have not been supported by larger studies. Alcohol, on the other hand, has been associated with many congenital deformities including CHDs. Some retinoids (aside from vitamin A) have associations with CHDs. Particularly, the drug Isotretinoin, which was previously prescribed for severe acne, is associated with CHDs as well as abnormalities in other organs including the thymus and eyes. There is an association between women who report working with organic solvents as part of their occupation and having children with CHDs, particularly ventricular septal defects (VSDs). One large registry study found that the use of nonsteroidal anti-inflammatory drugs has an association with CHDs (Ericson and Kallen, 2001). If the mother contracts *Rubella* during pregnancy, it can

spread to the fetus and cause CHDs and other developmental defects. Supplementation with folic acid is important for both proper neural tube closure and cardiac formation (Jenkins et al., 2007).

Lastly, some CHDs have been found to have genetic origins. Children with a chromosomal abnormality (such as trisomy 21 or trisomy 18, 22q11.2 deletion, and trisomy 13) have an increased risk of CHDs (Hartman et al., 2011). However, identifying the specific genes that, upon their deletion or duplication, cause the CHD in these syndromes can be problematic because a multitude of genes are misregulated in chromosomal abnormalities. On the other hand, there are many single genes involved in the development of the heart that have mutations known to cause CHDs. These mutations directly impact the heart or the vasculature of a developing embryo and will be discussed later.

It is clear from previous studies that improper formation of the heart occurs through a complex interplay of environmental and genetic causes. While these causes are known to affect heart development, a significant portion of CHDs have no detectable cause (Patel and Burns, 2013). Thus, more studies need to be done to reveal how CHDs arise. Insight in this area can be provided by understanding how normal heart development occurs.

Vertebrate heart development

The vertebrate heart is essential for the delivery of oxygen and nutrients as well as movement of metabolic waste products out of tissues. In very early stages, embryonic tissues are thin enough for this process to occur via diffusion. However, as the embryo

grows, simple diffusion is not sufficient. As such, the heart becomes the first functioning organ in the embryo to facilitate the distribution of these substances (Udan et al., 2013).

In mice, heart development begins with the specification of heart cell precursors—a tissue called the cardiogenic mesoderm—that forms from the medial lateral-plate mesoderm at embryonic day E6.5 (6.5 days after fertilization) (Saga et al., 1999). The cardiogenic mesoderm (or the heart field) of vertebrates forms during gastrulation (before lateral-plate mesoderm forms). Eventually, these cells reach the inside of the embryo in a location close to the pharyngeal arch, where they become specified into two separate fates: first heart field and second heart field. Cells of the first heart field leave the lateral-plate mesoderm (on both the left and right sides of the body) and these cells undergo mesenchymal to epithelial transformation on either side of the midline forming two heart tubes. Next, cells of the second heart field incorporate into the tubes, and the tubes fuse together at the midline to create a structure called the heart tube. The heart tube at this point is comprised of an inner lining of endocardial cells surrounded with contractile cells called cardiomyocytes (Buckingham et al., 2005). Cardiomyocytes make up the myocardium of the heart, and these are identifiable by the appearance of smooth muscle α-actin expression (Clement et al., 2007; Potta et al., 2010). The incorporation of second heart field cells into the initial heart tubes is not uniform, as the first heart field primarily gives rise to the left ventricle, and the second heart field primarily gives rise to the right ventricle, left and right atria and the outflow tract (OFT) (Rochais et al., 2009).

After the heart tube forms, the heart undergoes morphogenesis to eventually form a four-chambered heart. This initiates around E8-9 in mice and between days 20-28 of

human gestation by undergoing looping. Nodal and Pitx2 are proteins that pattern the left and right sides of the embryo. These proteins control which direction the heart will loop by acting as transcription factors regulating the expression of genes associated with the cytoskeleton (e.g. actin) (Noel et al., 2013). Prior to looping, both Hand1 and Hand2 are located throughout the heart tube pericardium. These proteins are controlled by Nkx2-5. Once the heart starts looping, Hand1 is exclusively expressed in the left ventricle, and Hand2 is expressed on the right side of the heart. The ventricles of the heart do not form as they should if any of these proteins are missing. Thus, looping is also impeded without these proteins (Biben and Harvey, 1997; Buckingham et al., 2005; Srivastava et al., 1995; Srivastava and Olson, 2000).

Other features of the heart formed during embryonic organogenesis include trabecula and septations, which help form the four chambers of the heart. Trabecula, found in the ventricles, are projections of the myocardium that form a mesh-like matrix on the inside of the heart. They start forming around E9.5 in mice (Captur et al., 2016). These formations are important for cardiac function as they help with strengthening and septating the ventricles, as well as acting as a precursor to the Purkinje fiber network of the cardiac conduction system (Granados-Riveron and Brook, 2012; Haack and Abdelilah-Seyfried, 2016; Niessen and Karsan, 2008; van Weerd and Christoffels, 2016).

Septations of the heart can be both thick and muscular as found between the left and right ventricles or membranous as occurs between the left and right atria. The ventricular septum begins to form around E11 in mice and starts on the inferior groove between the right and left ventricles. An equal portion of cells from both chambers proliferate upwards, creating the full septation by E12.5 (Christoffels et al., 2000;

Harvey, 2002). Unlike the ventricles, the atria of the mammalian heart are not fully separated until birth. This occurs due to a change in pressure when the first breath is taken. During development, the septum primum and the septum secundum form to partially form between the left and right atrium. They are not completely connected, but have a space called the foramen ovale to direct the flow of blood that is partially oxygenated from the placenta from the right atrium to the left atrium until birth. (Dalgleish, 1976; Kijima et al., 2017).

Lastly, the valves of the heart found at the outflow tract and at the atrial-ventricular junctions are needed to prevent backflow of blood. The valves are derived from endocardial tissue, specifically structures called the endocardial cushions. The endocardial cushions are made of an extracellular matrix called the cardiac jelly, which contains endothelial cells that undergo endothelial to mesenchyme transdifferentiation (EMT). These cells proliferate and migrate to form the valves. Signals identified in this process include (VEGF) for proliferation; NFATc1 in the endocardial cushions as a transcriptional regulator; Notch, Wnt/β-Catenin, and BMP/TGF-β for EMT; ErbB seems to regulate proliferation of the cells making up the valves; and NF1/Ras function to control EMT (Armstrong and Bischoff, 2004).

For each aspect of heart morphogenesis (looping, trabeculation, septation, chamber formation, and valve formation), a complex interplay of signals must be involved. To elucidate genetic signals, mutations in various genes have revealed impairment of proper heart morphogenesis leading to a CHD. These studies thus reveal critical genes that are involved in proper heart formation.

Genetically Generated Congenital Heart Defects

Many cases of CHDs in humans are linked to mutations in genes that are directly involved with heart development. Among these are *NKX2.5, GATA4, TBX5, TBX20, SALL4, ZIC3, TFAP2B, FOG2,* and *TBX1* (Clark et al., 2006; Garg et al., 2003). These genes are all transcription factors that regulate heart development. Some of these genes work together to either activate or repress certain genes, like *TBX5* and *SALL4*. As a result of this overlapping, the patterns of gene expression controlling heart development are quite complex (Bruneau, 2008).

To determine whether mutations in these genes are causative of CHD formation, researchers rely on information gleaned from model organisms. Mutation in many of the aforementioned genes in mice, for example, result in CHD formation. Mice that are homozygous mutant for *Nkx2.5* mice exhibit arrest of cardiac development after looping (Tanaka et al., 1999). Also, *Gata4* knockout mice reveal CHDs characterized by impaired looping, septation, and a hypoplastic ventricle (Watt et al., 2004). Thus, there are clearly specific mutations in genes that directly cause CHD formation; however, this is only part of the story.

In addition to mutations in genes that control heart development, CHD formation has been linked to mutations in genes that are required for cardiac contractility. There are various examples of these genes across different species. In humans, *α-Cardiac actin (ACTC1), α-Cardiac myosin heavy chain (MYH6)*, and *α-Cardiac myosin heavy chain (MYH7)* are mutations that have been linked to CHDs (Granados-Riveron and Brook, 2012). Mutation of cardiac contraction genes also give rise to CHDs in zebrafish (*cardiac troponin T* [*tnnt2*], *sarcomeric actin* [*cfk*], and *atrial myosin heavy chain* [*amhc*],

(Bartman et al., 2004; Berdougo et al., 2003)), chickens (*atrial myosin heavy chain* [*MYH7*] (Rutland et al., 2009)), and mice (*Myosin light chain 7* (*Myl7*) (also known as *Myosin light chain 2a* [*Mlc2a*]), *Cardiac troponin T* (*Tnnt2*), and *Na2-Ca2 exchanger* (*Ncx1*) (Anderson et al., 2015; Cho et al., 2000; Huang et al., 2003; Nishii et al., 2008). These mutations lead to a complex pathogenesis that is difficult to elucidate because in addition to affecting cardiac contractility directly, they also affect hemodynamic forces of blood flow, which may also be required for normal heart development (see below).

There are several pieces of evidence that implicate hemodynamic force in normal heart development. For example, there are also many genes involved in sensing sheer stress or acting in cell to cell communication that cause CHDs. Also, mutations that affect blood vessel development directly can be comorbid with impaired heart development. For example, vascular-specific alterations in Notch signaling (using *Tie2-Cre*) in the mouse is known to impair vascular development. For instance, vascular loss of Notch1 results in a failure for vessels to remodel (Limbourg et al., 2005), and activation of Notch1, via overexpression of Notch1-intracelullar domain (N1ICD), results in the presence of large sinusoidal vessels that also do not remodel (Copeland et al., 2011). In these same studies, vascular Notch1 inactivation also resulted in hearts with a thin myocardial wall and delayed looping; whereas, hyperactivation of Notch1 resulted in enlarged hearts. One interpretation of the observed heart defects is that the improperly remodeled blood vessels lead to an increase in resistance of blood flow, and as a result, the impaired blood flow may cause a secondary defect in heart development. The major caveat to interpreting these studies in this way is that the *Tie2-Cre* transgene is also expressed in the inner lining of the heart (the endocardium). Thus, these studies do not reveal if altered

Notch activity affects heart development directly or indirectly, and more studies should be done to elucidate the effect of altered flow dynamics on heart development.

CHDs generated by mechanical changes in hemodynamics

Various mechanical studies in fish and bird models implicate that alterations in hemodynamic force can affect heart development. A study in zebrafish manipulated hemodynamic force of 37 hours post fertilization (h.p.f.) embryos by inserting glass beads in the inflow and outflow tracts of the developing hear tube (Hove et al., 2003). This study found that by 4.5 days post fertilization (d.p.f.), obstructed blood flow at both the inflow and outflow tracts prevented looping and proper formation of the ventricle and atrium. There have been many studies that manipulate the hemodynamic loading of the chick embryonic heart (Midgett and Rugonyi, 2014). One way this has been accomplished is via ligation of the vitelline vein, the vein that returns blood to the chick heart. In one such study, a microclip was added to the right lateral vitelline vein of a stage 17 (70 hour incubated) chicken embryo *in ovo* and then incubated until stage 24 or 34 (26-122 hours). The 24 stage embryos exhibited looping defects and some hypoplasia of the endocardial cushions (Broekhuizen et al., 1999). Many of the embryos incubated to stage 34 had ventricular septal defects and semilunar valve defects. Another study induced a hypoplastic left heart (HLH) in chicken embryos by ligating the left atrium (deAlmeida et al., 2007). They found it was possible to rescue the HLH chicks by also ligating the right atria to increase the loading in the left ventricle.

There has been little done to assess the effect of mechanical manipulations of hemodynamic force on embryonic mouse hearts. This is due to the challenges of

culturing mouse embryos *ex vivo* along with the difficulty of manipulating these embryos. Mechanical studies conducted thus far have mainly examined the impact on vasculature and not the heart. One study assessed how ligating the left sixth branchial arch artery of an E11-11.5 mouse embryo compares to the right, non-ligated sixth branchial arch artery after culturing for 36 hours. They noted there was regression in the left sixth branchial arch artery compared to the right (Yashiro et al., 2007). Another study found that hemodynamic forces influence the development of the vasculature of the yolk sac in mice (Lucitti et al., 2007). In that study, the hematocrit was reduced in 5 somite stage mouse embryos by retaining blood cells in the yolk sac (the initial site of erythrocyte generation) with polyacrylamide and cultured for 24 hours. This lowered the hemodynamic force in a way that prevented remodeling of the yolk sac vessels. By administering hetastarch, which acts as a blood thickener, increasing hemodynamic force, to reduced hematocrit embryos prior to culturing, remodeling of the yolk sac vessels was rescued. This also revealed that remodeling failure upon reduction of hematocrit was not caused by improper oxygenation, as the rescue experiment does not provide back extra oxygenation.

Hypothesis

Taken together, these studies in zebrafish and chicken embryos have implicated that hemodynamic force is a factor that controls heart development. The role of hemodynamic force is not limited to avia or teleosts, as mouse embryonic vessels are also regulated by force. Thus, I have hypothesized hemodynamic force plays a role in mouse embryonic heart development. I studied this by applying the same mouse embryo culture

and hemodynamic force manipulation methods as described in (Lucitti et al., 2007). The focus for this study was on what happens to mouse embryonic heart development when hemodynamic force is reduced via retaining the blood cells in the blood islands of the yolk sac.

METHODS

Experimental design

Because mammalian embryos develop in utero, this limits accessibility of embryos for a whole host of experiments, including visualizing development, performing transplantation or extirpation studies, fate mapping, or other ways of manipulating embryos. To perform these experiments, the embryos must be removed from the uterus and cultured externally. Both preimplantation and post implantation embryos (up to E10.5) can be cultured externally for up to 24 hours (sometimes longer), though different culturing approaches (media, gaseous phases, or removal of yolk sac) may be needed depending on what stage the embryos are extracted from the mother. In this study, embryos were removed at E8.5, and cultured using techniques highlighted below.

Procedures

Mouse line and maintenance. CD1 mice with an *Myl7* null mutation were maintained according to Institutional Animal Care and Use Committee (IACUC) protocols established by Missouri State University (November 20, 2014; approval #15-004.0-A, December 01, 2014; approval #15-008.0-A). For embryo manipulation studies, only CD1 mice that were homozygous for the wild type allele of *Myl7* were used. Breeding mice in this way ensures that I efficiently uses this mouse line (as per IACUC rules) while retaining the *Myl7* mutation for other experiments (such as for the developmental delay experiment). Animals were housed according to the guidelines set by the National Institutes of Health (NIH). The mice were kept in a room at ambient

temperature (23-26 °C) on a 12 hour day/night cycle starting at 7 A.M. All adult mice were maintained on a diet of Purina Labdiet 5001 in a clean standard shoebox cage (Ancare) with *ad libitum* access to food and water. However, if the mice were used for breading or experiments, they were fed Purina Formulab diet 5008.

For embryo manipulation studies, *Myl7*$^{+/+}$ (CD1 background) male and female mice were crossed, and the female was checked every morning for a vaginal plug. The day a plug was present was considered embryonic day 0.5 (or E0.5). The dissection of these embryos was done on E8.5.

Mouse genotyping. To verify the genotype of the animals used, tissue samples for genotyping were collected from tail tips of recently weaned and tattooed mice, or from embryos. If adult mice needed to be genotyped, they were anesthetized with 3 ppm isoflurane before collecting a tissue sample from the tail.

Tail cuts from weaned or adult mice were digested in 200 µl of tail buffer (TLB, 0.1M NaCl, 0.05M Tris [pH 8.0], 0.1M EDTA [pH 8.0], 5 ml 10% SDS, q.s. to 50 ml) and 10 µl Proteinase K (Thermoscientific, #EO0491, Lot 00323614) overnight at 55 °C. The next day, DNA was extracted by adding 200 µl of phenol chloroform (Fisher Scientific, BP1753I-100), mixing by inversion, followed by centrifugation at 17.0 Xg for 10 minutes. The upper phase (180 µl), containing the DNA, was removed and placed in a clean microcentrifuge tube. Isopropanol (180 µl) (Fisher Scientific, Cat. A461-500) was added to precipitate the DNA. The DNA was pelleted via centrifugation and the isopropanol was removed. A wash of 500 µl of 70% ethanol (Fisher BioReagents™, Cat. BP28184) was added and the tube was centrifuged again. Next, the ethanol was removed

and allowed to evaporate. The DNA was then suspended in 75 µl of distilled water and stored at 4 °C until needed for polymerase chain reaction (PCR).

For the PCR, each reaction had 39 µl of master mix (15 µl distilled water, 2 µl of forward primer, 2 ul of reverse primer, and 20 µl Taq Pro Red Complete [Denville Scientific Inc., Lot BMR15-616110]) and 1 µl of DNA. Adult mice can only be homozygous wild type for the *Myl7* gene, or heterozygous because *Myl7*$^{-/-}$ homozygous mutants are embryonic lethal by E10.5-E11.0. Thus, genotypes for adult mice were determined by detecting the null mutation by PCR. Specifically, the null mutation would be present if a 763bp PCR fragment forms using the following primers: *Myl7* Mut-F (DNA sequence: 5′- ACAGGGAATCACA-3′), 2 µl *Myl7* Mut-R (DNA sequence: 5′-CGAACCTGGTCGA-3′). For genotyping embryos, presence of the mutation was detected, as previously mentioned, and presence of the wild type *Myl7* allele was detected using *Myl7* Wt-F (DNA Sequence: 5′-GGCACGATCACTC-3′), and *Myl7* Wt-R (DNA sequence: 5′-ATCCCTGTTCTGG-3′) primers. The expected band for presence of the wild type allele is a 590bp fragment. The PCR was done with a TECHNE, 3PRIMEBASE/02 using the following parameters: 95 °C for 5 minutes, 35 cycles (95 °C 30 seconds, 56.5 °C for 30 seconds, 72 °C for 1 minute), 72 °C for 5 minutes, and 4 °C. Samples were run on an electrophoresis gel (2% agarose, with 12 µl ethidium bromide) with a DNA ladder (MidSci, Bulls eye, lot200217). The gel was imaged with a Gel Imaging System (Azure Biosystems, c300) and presence of the *Myl7* mutation was assessed.

Rat serum collection. Sprague-Dawley rats (about 7 weeks old, initially from Charles River, but bred in house) were anesthetized with diethyl ether (Acros Organics,

Cat. 123990010) in a desiccator (Fisher: 08 615B). Unresponsive rats were removed from the chamber and placed in supine position, and tested for adequate depth of anesthesia by assessing pedal withdrawal and palpebral reflexes. The nose and mouth were covered with a 50 ml Falcon tube containing an ether-soaked Kimwipe (Kimberly Clark Science brand) to ensure anesthetization during the procedure. The peritoneal cavity was opened, the organs were moved aside, and the viscera was moved away to expose the dorsal aorta. A BD Vacutainer® Safety-Lok™ Blood Collection Set (BD Medical Supplies, Ref 367283) needle was inserted into the dorsal aorta and blood was drained into a BD Vacutainer SST™ Plus Blood Collection Tube (BD Medical Supplies, Ref 367985) that was inverted to mix in the anticoagulants. Euthanasia was completed by decapitation with a guillotine (Braintree scientific: NS-80-2).

The blood collection tubes were then centrifuged at 13.0 xg for 20 minutes to purify the serum. All serum was then sorted into 15 ml Falcon tubes (MidSci, C15R) based on purity. High quality serum was labeled “clear”, followed by “medium”, and lastly serum containing a high proportion of lysed red blood cells labeled “pink”. These tubes were then centrifuged at 1300 RCF for 10 minutes to pellet any remaining blood cells. The serum was then decanted into three 50 ml Falcon tubes (MidSci, Cat. C50R, labeled “clear”, “medium”, and “pink”). These tubes were covered with a Kimwipe and placed in a 56 °C water bath for 30 minutes to heat inactivate the serum and allow the ether to evaporate. The tubes were then moved to 4 °C overnight to further evaporate the ether.

The next day, all serum was sterile filtered (Fisher Brand, Cat. No 09-719D) and 1 ml of serum was aliquoted to 1.5 ml centrifuge tubes labeled with the date and quality. These were then stored at -80 °C for up to a year.

Embryo culture. The night before dissection, two 1 ml aliquots of clear rat serum were removed from storage at -80 °C to allow dissipation of ether from the serum. Each of these tubes were opened, placed in loosely capped 50 ml Falcon tubes, and stored at 4 °C until the next day.

On the day of the dissection, dissection media containing 25ml of Dulbecco's Modified Eagle Medium (Gibco® by Life Technologies™, REF 11330-032) supplemented with 5 ml fetal bovine serum (Gibco) and 0.5 µl of penicillin/streptomycin (Sigma, P4458-100ML) was made in sterile conditions.

The loosely capped rat serum and dissection media tubes were placed in an incubator (Fisher Scientific™ Isotemp™ CO_2 Incubator, Cat. 13-255-27) maintained at 37 °C with 5% CO_2 (Airgas, Randor, PA). About 1-2 ml of dissection media was placed in two 60 mm x 15 mm petri dishes (Fisherbrand™, Cat. FB0875713A) and eight 35 mm x 10 mm petri dishes (Falcon®, REF 351008). Everything was left in the incubator for at least an hour before the dissection.

After the dissection and manipulation(s), embryos were allowed to equilibrate for an hour. During this time, two aliquots of culture media (1:11 ml rat serum to dissection media) were made in 50 ml Falcon tubes and gassed (Airgas, bloodgas mixture) for 3 minutes to remove any remaining ether from the rat serum, and to balance the gaseous phase of the culture media. The culture media was emptied into 60 mm x 15 mm petri

dishes and allowed to equilibrate in the incubator for 1 hour. Embryos were then transferred into the respective plates and kept there for 24 hours.

Dissection. Mice 8.5 days into pregnancy were sacrificed with CO_2 and cervical dislocation. The peritoneal cavity was opened and one at a time, the uterine horns were removed. Incisions were made in the myometrium between each embryo to reduce tension of the contractions before moving to dissection media. The uterine horn was then placed in a 60 mm x 15 mm petri dish with dissection media (previously described). This dish was moved to the stage of a dissection microscope (AmScope, SM-1TSZ-L6W) surrounded by a homemade heater box (cardboard box with front cut out and covered in insulating material attached to a heater that maintains the temperature at 37 °C).

Next, the embryos were completely cut apart and the myometrium was removed. Embryos were then moved to 35 mm x 15 mm culture dishes (no more than 4 per dish) filled with dissection medium and placed in the incubator. The decidua and parietal yolk sacs were carefully removed from one petri dish of embryos at a time, while keeping the visceral yolk sac and ectoplacental cone intact. These embryos were then transferred to a new 35 mm x10 mm culture dish with dissection media and stored in the incubator and the rest of the embryos were dissected.

Microinjections. In Lucitti et al., 2007, a low hemodynamic force embryonic mouse model was created by preventing blood cells from leaving the blood islands; hence, these embryos were referred to as “reduced-hematocrit” embryos. By reducing hematocrit, this diminishes the amount of hemodynamic force that is normally provided by the high viscosity that blood cells create in flowing blood. In my thesis study, reduced-hematocrit embryos will be referred to as “low-hemodynamic loading” embryos

because it also has an effect of minimizing the amount of hemodynamic force that the heart is exposed to, as well as the amount of effort that the heart exerts in pumping blood.

To make low-hemodynamic loading embryos, the yolk sac blood islands (where the pre-circulatory blood cells reside) must be injected with substances that prevent their entry into circulation. The substances used were Acrylamide (450 µl 2x PBS, 250 µl of DiH_2O, 250 µl 30% Bis-acrylamide [Fisher Scientific, Cat. No. BP1366]), 50 µl India ink [American MasterTech, REF STIIN25], 20 µl 0.5 M ammonium persulfate [Thermo Scientific, CAS: 7727-54-0]) and TEMED (50 µl TEMED [Fisher BioReagents, CAS 110-18-9], 50 µl 2x PBS, 2 µl India ink). The acrylamide and TEMED solutions were centrifuged at 17.0 xg for 1 minute and then sterile filtered to avoid clogging the very thin microinjection needle. The experimental embryos were injected with both acrylamide and TEMED (AT) into the blood islands resulting in low hemodynamic loading embryos (because blood cells failed to enter circulation). For one category of control embryos, only the solution of acrylamide (Ao) was injected into the blood islands, and blood cells still entered circulation. For N control embryos, no injections were performed and these embryos were transferred to culture media at the same time as the AT and Ao embryos (Fig. 1).

In embryos 8 somites and younger, the flow of blood in the yolk sac blood islands is so low that the acrylamide, TEMED, and blood cells remain in these areas once polymerized. However, after 8 somites the blood cells begin to enter circulation. Thus, embryos used for injections were between 4 and 6 somites.

Acrylamide injections were done in the proximal yolk sac blood islands 2 to 3 times in 3 to 4 sites of the blood islands. After the acrylamide injections, the embryos

were replaced in the incubator to equilibrate for 15 minutes. Then (for AT embryos), a similar amount of TEMED was injected at the same injection sites as the acrylamide. Embryos were then transferred to culture media to culture for 24 hours.

Needles used for injection were made using 0.4 mm I.D. length 75 mm capillary tubes (Drummond Scientific Co., Cat. # 1-000-800) pulled on a PMP-102 Micropipette Puller (MicroData Instrument, Inc., PMP-102) set on the preprogrammed sequence SQ20 for a taper length of 3 mm, an outer diameter of 2-20 μm, and a tip opening of <1-2 μm.

Injections into the proximal yolk sac blood islands were performed with a Pico-Liter Injector (Warner Instruments, PLI-10) set at 3 PSI With an injection time of 0.10 seconds.

Heart staining and OPT processing. After culturing for 24 hours, viability of the embryos was determined. Though most control embryos used for this study were with injections with acrylamide alone, TEMED only injections have been tested before, and these did not appear to have any difference in health of the embryos similar to acrylamide injections. Health of the embryo was determined by assessing several factors: 1) continued cardiac contraction and blood flow; 2) remodeling of the yolk sac vasculature; 3) analysis of extent of embryogenesis (i.e., the embryo undergoes turning, somitogenesis, growth, etc.). Thus, controls exhibited healthy heart contractility, blood flow, vascular remodeling, and embryogenesis. For experimental embryos, I discarded embryos that retained blood cells in circulation, or had blood cells that did enter circulation, but pooled in the vessels. However, I did use experimental embryos that exhibited no blood cells in circulation, no remodeling of the yolk sac vessels, continued cardiac contractility, and similar somitogenesis.

Control and experimental embryos (in the yolk sac with the ectoplacental cone punctured) were then fixed in 4% paraformaldehyde (Fisher Scientific, CAS No. 30525-89-4) for one hour. After fixing, the PFA was removed and the embryos were washed three times in fresh 1x PBS, then stored in 1% sodium azide (Fisher Scientific, CAS NO. 26628-22-8)

The embryos were blocked with 200 µl of serum blocking buffer (SBT, 1x PBS, 2% normal donkey serum [Sigma-Aldrich, Cat. D9663-10ML], 0.8% Triton X [Fisher Scientific, CAS No. 9002-93-1]) for 1 hour and then stained with 1:250 anti-α-actin smooth muscle Cy3 (Sigma-Aldrich, Cat. C6198-.2ML) in SBT, which is transiently expressed in the heart at this stage. They were then washed with 1x PBT (0.8% Triton) and then stored in 1% sodium azide at 4 °C until somite counting. The yolk sacs and amnion were removed from the embryos for somite staging before processing for optical projection tomography.

After staining, the embryos were prepared for imaging with OPT. First, they were embedded in 1% agarose in 1x phosphate buffer solution (PBS). This was done by immersing the embryos in the agarose solution and aspirating it into a cut off pipette tip. While cooling, the pipette was manually rotated to center the embryo in the agarose. Once completely cooled, the agarose was removed and the section containing the embryo was cut away and placed in a dehydrating solution of 25% methanol (Fisher Scientific, CAS 67-56-1) in 1x PBS in a 15 ml centrifuge tube (MidSci, Cat. C50R). Complete dehydration of the embryos was accomplished by replacing the solution every 24 hours with 50%, 75%, 100%, and 100% methanol in 1x PBS solutions. Next, the embryos and agar were cleared with a 1:2 solution of Benzyl Alcohol (Fisher Scientific, A396-500) in

Benzyl Benzoate (Acros Organics, CAS 120-51-4) (BABB). After clearing overnight, the BABB wash was replaced with fresh BABB for storage and imaging.

Imaging samples with OPT. Samples were imaged on a custom-made optical projection tomography (OPT) microscopy system at Baylor College of Medicine courtesy of Dr. Mary Dickinson's lab. The OPT is made up of an excitation light source (with a 531 nm filter for our purposes), a magnetic and motile sample stage, an emission filter of 593 nm, and a camera (Fig. 2). The embryo mounted to a rotating metal chuck (that is magnetized to the rotating stage) suspended in a basin of BABB. A 2D image of the emitted light was collected every 0.3 degrees the embryo was rotated.

Images collected from the OPT were aligned using NRecon to construct a 3D image of the heart. These files were then compatible with Imaris, a software program I used for data collection.

Data collection

To minimize the effects of age difference on the statistical analysis embryo hearts, the embryos were grouped in ranges of 3 somite pairs: <14, 14-16, 17-19, 20-22, and 23-25. Unfortunately, enough samples were generated for only the 14-16 and 17-19 somite ranges. (Table 1).

To assess the size of mouse embryo hearts, we looked at the volume contained by the myocardium. These measurements were obtained by outlining the inside of the myocardium throughout the 3D heart, including the trabecula (Fig. 3). The volume contained by the selection was calculated by Imaris and recorded.

The myocardial thickness was assessed by taking four measurements of the myocardium excluding the trabecula (Fig. 4) on five sections along the heart: one near the inflow tract, one near the outflow tract, and the other three were evenly spaced between the sections near the inflow and ouflow tracts.

Statistical tests were performed using the two sample t-test in R, with a significance level of $P < 0.05$. The number of samples produced for each condition (n) are listed in Table 1.

RESULTS

After culturing the AT (Acrylamide and TEMED-injected) embryos for 24 hours, visual inspection of the AT embryos revealed the presence of heart contractions; however an absence of blood cells entering in circulation. This resulted in a lack of vascular remodeling of the yolk sac due to the reduction in hemodynamic force. Whereas, the N and Ao embryos did exhibit heart contractions, blood flow, and normal vascular remodeling—indicating that hemodynamic force is very high in these embryos. Embryos that were collected at E8.5, before they were manipulated, generally ranged from 4-6 somites (before blood cells enter circulation). After approximately 24 hours of culturing, there was some variability in the stage of development that has been attained. Mostly, the 14-16 somite or 17-19 somite groups had a sufficient amount of embryos for statistical analysis across all treatment groups (Table 1).

Past studies have indirectly assessed stroke volume (Broekhuizen et al., 1999) and ejection volume (Hove et al., 2003) of the heart. Broekhuizen et al., 1999 found that there may be a compensatory mechanism increasing stroke volume in stage 34 chick embryos with ligation of the right lateral vitelline vein. The ejection volume in Hove et al., 2003 was calculated to determine that the shear forces acting on the cardiac endothelial cells were significant. These studies approximate the volume of blood the heart expels. Unfortunately, such approximations cannot be obtained for the study as processing for OPT necessitates fixation of the embryos. However, the high resolution of the OPT does allow for direct measurements for the morphological volume. As such, direct measurements of the heart volume were successfully obtained using Imaris (as described

in Methods). Qualitative comparison of 3D images of the hearts between the AT (reduced hemodynamic loading) and the control embryos (N and AO) showed a lot of variability in sizes, even between embryos of the same somite stage group. So, statistical evaluation was needed to determine if there was a difference. Statistical analysis of the embryonic heart volumes revealed that there was no significant difference in the heart volumes between the AT (reduced hemodynamic loading) embryos and the control embryos (N and Ao) (Fig. 5; Fig. 6).

Although there was no observable change in the heart volume when hemodynamic forces are reduced, measurements for volume were taken of the lumen of the heart itself (i.e., it did not include the myocardium). Thus, there could still be a change in thickness in the myocardium that I would not have been able to detect when I assessed heart volumes. It is possible that the thickness of the myocardium could be influenced during our culturing period because cardiomyocytes do proliferate between E8.5 and E9.5 (Zhao and Rivkees, 2003). Myocardial thickness was measured at multiple locations of the myocardium along the heart tube as described in methods. Statistical tests revealed a significant decrease in the myocardial thickness in AT embryonic hearts as compared to both of the controls at the 14-16 and 17-19 somite stages (Fig. 7; Fig. 8).

DISCUSSION

Summary

Considering that reduction of hemodynamic force (or hemodynamic loading in the heart) in reduced-hematocrit mouse embryos has been show to prevent blood vessels from properly remodeling, I expected that this could also impact development of the heart. This was further corroborated by other studies in zebrafish and chicken embryos where alterations in hemodynamic loading do result in a change in heart morphology (deAlmeida et al., 2007; Hove et al., 2003; Sedmera et al., 1999). When using OPT imaging to obtain high resolution 3D images of the mouse embryonic hearts, and by performing morphometric analysis, I were able to observe a small, but significant difference in myocardial thickness between low-hemodynamic loading embryos and controls, with no significant difference in total heart volume detected.

The slight decrease in myocardial thickness observed in the low hemodynamic force embryos compared to embryos with normal hemodynamic force is in line with other studies showing stunted cardiovascular development with reduced blood forces (Anderson et al., 2015; Granados-Riveron and Brook, 2012; Hove et al., 2003; Lucitti et al., 2007; Sedmera et al., 1999). The reason for this may be that force sensing factors in the heart that signal cardiomyocyte proliferation are not being turned on. Notch signals are known to induce development of the vasculature in a hemodynamic force-dependent manner (Anderson et al., 2015). It is possible these or similar signals also play a role in the development of the heart itself.

There are a couple of possible explanations for the lack of change in the heart volume: First, reduced hemodynamic loading does not affect heart volume (E8.5 to E9.5), and second the statistical power was not high enough to show a difference. The second explanation suggests that there could be a difference that is not detectable because our n-value is too low. The reason for the low n-value was due to a combination of factors. First, litter sizes vary and some mice do not produce enough embryos. Second, the experiments depend on success of the dissections, injections, and culture. Performing these delicate procedures have a very long learning curve. Third, it is possible there is a developmental delay in the AT embryos that will be discussed later. These aspects of this project resulted in a long process of producing embryos for this experiment, leading to the low n-value. However, even with the low n-value, the number of embryos used for this study was very close to comparable studies (Anderson et al., 2015). Therefore, it is highly doubtful that adding more embryos to the study will reveal a significant difference in volume since there was so much variability seen from embryo to embryo (even within the same somite group).

In conclusion, there was no observable difference in heart volume of mice cultured from E8.5 to E9.5 with reduced hemodynamic force compared to normal mice with normal hemodynamic force. A slight decrease was observed in the myocardial thickness between mice with reduced hemodynamic force and the control mice. It is possible that decreased homodynamic force has other implications in heart development. There are other aspects of heart development that can be assessed with this data set, but are not included in this study due to time constraints.

Future Direction

One aspect of heart development that was not assessed in this study is the role lowered hemodynamic force plays in the development of trabecula. Trabecualtion does not occur in zebrafish when there are mutations in genes that decrease blood flow in the ventricles (Haack and Abdelilah-Seyfried, 2016). Trabecula were observed in the hearts generated for this study (Fig. 3A). Therefore, an assessment of their development is warrented.

Another event in heart development that can be investigated with this data set is to determine if low hemodynamic force impacts looping. Mice with mutations in *DLL4*, which plays a role in vascular development) have less looping of the heart tube (Anderson et al., 2015). As such, the extent of looping in the low hemodynamic force embryos vs. the control embryos needs to be determined.

Since there seemed to be a delay in the somitogenesis of the AT embryos compared to the controls, as there was a singular embryo produced that was more than 19 somites in the AT group, one thing that can be assessed is whether or not mutations that reduce hemodynamic force are also delayed. This may be corroborated by assessing somitogenesis in *Myl7* mutant strain, which presents decreased homodynamic force due to decreased contractility in the atria that effects heart development (Anderson et al., 2015; Culver and Dickinson, 2010; Lucitti et al., 2007).

This study looked at embryos in static culture from E8.5 until E9.5. In Lucetti et al. 2007, they used roller culture. This helps circulate the nutrients and wastes in the medium and allows for more robust growth of the embryo vs. static culture. Other studies have cultured embryos from a more advanced age (E11) and longer (36 hours) (Yashiro

et al., 2007). If embryos at E11 and beyond are to be assessed, alternative mechanical manipulations of hemodynamic force may need to be explored as hematopoiesis begins in the liver at that stage (Conrad et al., 2004).

One study observed that ligating the left sixth brachial arch artery (BAA) on the BAA and the dorsal aorta at E11.5 lead to regression of the left BAA (Yashiro et al., 2007). While this study did not assess heart development, it is possible that an atrial ligation similar to that in chick embryos (Hove et al., 2003) at this E11.5 stage may provide insight on hemodynamic forces in heart development. In the study by Yashiro et al., 2007, they also looked at how propranolol (a β-adrenergic antagonist that decreases heart rate) effected the development of the BAA. Treating embryos with this or other drugs that influence heart rate are also possible ways to see if hemodynamic forces are important for heart development.

REFERENCES

Anderson, G.A., Udan, R.S., Dickinson, M.E. and Henkelman, R.M., (2015). Cardiovascular patterning as determined by hemodynamic forces and blood vessel genetics. *PloS one* **10**, e0137175.

Armstrong, E.J. and Bischoff, J., (2004). Heart valve development: Endothelial cell signaling and differentiation. *Circulation research* **95**, 459-470.

Bartman, T., Walsh, E.C., Wen, K.K., McKane, M., Ren, J., Alexander, J., Rubenstein, P.A. and Stainier, D.Y., (2004). Early myocardial function affects endocardial cushion development in zebrafish. *PLoS biology* **2**, E129.

Berdougo, E., Coleman, H., Lee, D.H., Stainier, D.Y. and Yelon, D., (2003). Mutation of weak atrium/atrial myosin heavy chain disrupts atrial function and influences ventricular morphogenesis in zebrafish. *Development* **130**, 6121-6129.

Biben, C. and Harvey, R.P., (1997). Homeodomain factor nkx2-5 controls left/right asymmetric expression of bhlh gene ehand during murine heart development. *Genes & development* **11**, 1357-1369.

Broekhuizen, M.L., Hogers, B., DeRuiter, M.C., Poelmann, R.E., Gittenberger-de Groot, A.C. and Wladimiroff, J.W., (1999). Altered hemodynamics in chick embryos after extraembryonic venous obstruction. *Ultrasound in obstetrics & gynecology : the official journal of the International Society of Ultrasound in Obstetrics and Gynecology* **13**, 437-445.

Bruneau, B.G., (2008). The developmental genetics of congenital heart disease. *Nature* **451**, 943-948.

Buckingham, M., Meilhac, S. and Zaffran, S., (2005). Building the mammalian heart from two sources of myocardial cells. *Nature reviews. Genetics* **6**, 826-835.

Bull, C., (1999). Current and potential impact of fetal diagnosis on prevalence and spectrum of serious congenital heart disease at term in the UK. *British Paediatric Cardiac Association. Lancet* **354**, 1242-1247 ik.

Captur, G., Wilson, R., Bennett, M.F., Luxan, G., Nasis, A., de la Pompa, J.L., Moon, J.C. and Mohun, T.J., (2016). Morphogenesis of myocardial trabeculae in the mouse embryo. *Journal of anatomy* **229**, 314-325.

Cho, C.H., Kim, S.S., Jeong, M.J., Lee, C.O. and Shin, H.S., (2000). The Na+ -Ca2+ exchanger is essential for embryonic heart development in mice. *Molecules and cells* **10**, 712-722.

Christoffels, V.M., Habets, P.E., Franco, D., Campione, M., de Jong, F., Lamers, W.H., Bao, Z.Z., Palmer, S., Biben, C., Harvey, R.P. and Moorman, A.F., (2000). Chamber formation and morphogenesis in the developing mammalian heart. *Developmental biology* **223**, 266-278.

Clark, K.L., Yutzey, K.E. and Benson, D.W., (2006). Transcription factors and congenital heart defects. *Annual review of physiology* **68**, 97-121.

Clement, S., Stouffs, M., Bettiol, E., Kampf, S., Krause, K.H., Chaponnier, C. and Jaconi, M., (2007). Expression and function of alpha-smooth muscle actin during embryonic-stem-cell-derived cardiomyocyte differentiation. *Journal of cell science* **120**, 229-238.

Conrad, M., Jakupoglu, C., Moreno, S.G., Lippl, S., Banjac, A., Schneider, M., Beck, H., Hatzopoulos, A.K., Just, U., Sinowatz, F., Schmahl, W., Chien, K.R., Wurst, W., Bornkamm, G.W. and Brielmeier, M., (2004). Essential role for mitochondrial thioredoxin reductase in hematopoiesis, heart development, and heart function. *Molecular and cellular biology* **24**, 9414-9423.

Copeland, J.N., Feng, Y., Neradugomma, N.K., Fields, P.E. and Vivian, J.L., (2011). Notch signaling regulates remodeling and vessel diameter in the extraembryonic yolk sac. *BMC developmental biology* **11**, 12.

Culver, J.C. and Dickinson, M.E., (2010). The effects of hemodynamic force on embryonic development. *Microcirculation* **17**, 164-178.

Dalgleish, A.E., (1976). The development of the septum primum relative to atrial septation in the mouse heart. *Journal of morphology* **149**, 369-382.

Daubert, M.A. and Jeremias, A., (2010). The utility of troponin measurement to detect myocardial infarction: Review of the current findings. *Vascular health and risk management* **6**, 691-699.

deAlmeida, A., McQuinn, T. and Sedmera, D., (2007). Increased ventricular preload is compensated by myocyte proliferation in normal and hypoplastic fetal chick left ventricle. *Circulation research* **100**, 1363-1370.

Ericson, A. and Kallen, B.A., (2001). Nonsteroidal anti-inflammatory drugs in early pregnancy. *Reproductive toxicology* **15**, 371-375.

Garg, V., Kathiriya, I.S., Barnes, R., Schluterman, M.K., King, I.N., Butler, C.A., Rothrock, C.R., Eapen, R.S., Hirayama-Yamada, K., Joo, K., Matsuoka, R., Cohen, J.C. and Srivastava, D., (2003). GATA4 mutations cause human congenital heart defects and reveal an interaction with TBX5. *Nature* **424**, 443-447.

Goldstein, S.R., (1994). Embryonic death in early pregnancy: A new look at the first trimester. *Obstetrics and gynecology* **84**, 294-297.

Granados-Riveron, J.T. and Brook, J.D., (2012). The impact of mechanical forces in heart morphogenesis. *Circulation. Cardiovascular genetics* **5**, 132-142.

Haack, T. and Abdelilah-Seyfried, S., (2016). The force within: Endocardial development, mechanotransduction and signalling during cardiac morphogenesis. *Development* **143**, 373-386.

Hartman, R.J., Rasmussen, S.A., Botto, L.D., Riehle-Colarusso, T., Martin, C.L., Cragan, J.D., Shin, M. and Correa, A., (2011). The contribution of chromosomal abnormalities to congenital heart defects: A population-based study. *Pediatric cardiology* **32**, 1147-1157.

Harvey, R.P., (2002). Patterning the vertebrate heart. nature reviews. *Genetics* **3**, 544-556.

Hoffman, J.I., (1995). Incidence of congenital heart disease: II. Prenatal incidence. *Pediatric cardiology* **16**, 155-165.

Hove, J.R., Koster, R.W., Forouhar, A.S., Acevedo-Bolton, G., Fraser, S.E. and Gharib, M., (2003). Intracardiac fluid forces are an essential epigenetic factor for embryonic cardiogenesis. *Nature* **421**, 172-177.

Huang, C., Sheikh, F., Hollander, M., Cai, C., Becker, D., Chu, P.H., Evans, S. and Chen, J., (2003). Embryonic atrial function is essential for mouse embryogenesis, cardiac morphogenesis and angiogenesis. *Development* **130**, 6111-6119.

Jenkins, K.J., Correa, A., Feinstein, J.A., Botto, L., Britt, A.E., Daniels, S.R., Elixson, M., Warnes, C.A., Webb, C.L. and American Heart Association Council on Cardiovascular Disease in the, Y., (2007). Noninherited risk factors and congenital cardiovascular defects: Current knowledge: A scientific statement from the american heart association council on cardiovascular disease in the young: Endorsed by the American Academy of Pediatrics. *Circulation* **115**, 2995-3014.

Keeley, E.C., Boura, J.A. and Grines, C.L., (2003). Primary angioplasty versus intravenous thrombolytic therapy for acute myocardial infarction: A quantitative review of 23 randomised trials. *Lancet* **361**, 13-20.

Kijima, Y., Bokhoor, P. and Tobis, J.M., (2017). Patent foramen ovale with right atrial septal pouch. *Catheterization and cardiovascular interventions : official journal of the Society for Cardiac Angiography & Interventions* **89**, E169-E171.

Limbourg, F.P., Takeshita, K., Radtke, F., Bronson, R.T., Chin, M.T. and Liao, J.K., (2005). Essential role of endothelial Notch1 in angiogenesis. *Circulation* **111**, 1826-1832.

Lucitti, J.L., Jones, E.A., Huang, C., Chen, J., Fraser, S.E. and Dickinson, M.E., (2007). Vascular remodeling of the mouse yolk sac requires hemodynamic force. *Development* **134**, 3317-3326.

Makikallio, K., Jouppila, P. and Rasanen, J., (2005). Human fetal cardiac function during the first trimester of pregnancy. *Heart* **91**, 334-338.

Midgett, M. and Rugonyi, S., (2014). Congenital heart malformations induced by hemodynamic altering surgical interventions. *Frontiers in physiology* **5**, 287.

Nassr, A.A., El-Nashar, S.A., Shazly, S.A., White, W.M. and Brost, B.C., (2016). Expected probability of congenital heart disease and clinical utility of fetal echocardiography in pregnancies with pre-gestational diabetes. *European journal of obstetrics, gynecology, and reproductive biology* **201**, 121-125.

Niessen, K. and Karsan, A., (2008). Notch signaling in cardiac development. *Circulation research* **102**, 1169-1181.

Nishii, K., Morimoto, S., Minakami, R., Miyano, Y., Hashizume, K., Ohta, M., Zhan, D.Y., Lu, Q.W. and Shibata, Y., (2008). Targeted disruption of the cardiac troponin t gene causes sarcomere disassembly and defects in heartbeat within the early mouse embryo. *Developmental biology* **322**, 65-73.

Noel, E.S., Verhoeven, M., Lagendijk, A.K., Tessadori, F., Smith, K., Choorapoikayil, S., den Hertog, J. and Bakkers, J., (2013). A Nodal-independent and tissue-intrinsic mechanism controls heart-looping chirality. *Nature communications* **4**, 2754.

Oster, M.E., Riehle-Colarusso, T., Alverson, C.J. and Correa, A., (2011). Associations between maternal fever and influenza and congenital heart defects. *The Journal of pediatrics* **158**, 990-995.

Patel, S.S. and Burns, T.L., (2013). Nongenetic Risk Factors and Congenital Heart Defects. *Pediatric cardiology* **34**, 1535-1555.

Potta, S.P., Liang, H., Winkler, J., Doss, M.X., Chen, S., Wagh, V., Pfannkuche, K., Hescheler, J. and Sachinidis, A., (2010). Isolation and functional characterization of alpha-smooth muscle actin expressing cardiomyocytes from embryonic stem cells. *Cellular physiology and biochemistry : international journal of experimental cellular physiology, biochemistry, and pharmacology* **25**, 595-604.

Rochais, F., Mesbah, K. and Kelly, R.G., (2009). Signaling pathways controlling second heart field development. *Circulation research* **104**, 933-942.

Rouse, B. and Azen, C., (2004). Effect of high maternal blood phenylalanine on offspring congenital anomalies and developmental outcome at ages 4 and 6 years: The importance of strict dietary control preconception and throughout pregnancy. *The Journal of pediatrics* **144**, 235-239.

Rutland, C., Warner, L., Thorpe, A., Alibhai, A., Robinson, T., Shaw, B., Layfield, R., Brook, J.D. and Loughna, S., (2009). Knockdown of alpha myosin heavy chain disrupts the cytoskeleton and leads to multiple defects during chick cardiogenesis. *Journal of anatomy* **214**, 905-915.

Saga, Y., Miyagawa-Tomita, S., Takagi, A., Kitajima, S., Miyazaki, J. and Inoue, T., (1999). MesP1 is expressed in the heart precursor cells and required for the formation of a single heart tube. *Development* **126**, 3437-3447.

Sedmera, D., Pexieder, T., Rychterova, V., Hu, N. and Clark, E.B., (1999). Remodeling of chick embryonic ventricular myoarchitecture under experimentally changed loading conditions. *The Anatomical record* **254**, 238-252.

Smithells, R.W. and Newman, C.G., (1992). Recognition of thalidomide defects. *Journal of medical genetics* **29**, 716-723.

Srivastava, D., Cserjesi, P. and Olson, E.N., (1995). A Subclass of bHLH proteins required for cardiac morphogenesis. *Science* **270**, 1995-1999.

Srivastava, D. and Olson, E.N., (2000). A genetic blueprint for cardiac development. *Nature* **407**, 221-226.

Tanaka, M., Chen, Z., Bartunkova, S., Yamasaki, N. and Izumo, S., (1999). The cardiac homeobox gene Csx/Nkx2.5 lies genetically upstream of multiple genes essential for heart development. *Development* **126**, 1269-1280.

Udan, R.S., Culver, J.C. and Dickinson, M.E., (2013). Understanding vascular development. *Wiley interdisciplinary reviews. Developmental biology* **2**, 327-346.

van Weerd, J.H. and Christoffels, V.M., (2016). The formation and function of the cardiac conduction system. *Development* **143**, 197-210.

Vargesson, N., (2009). Thalidomide-induced limb defects: Resolving a 50-year-old puzzle. *BioEssays : news and reviews in molecular, cellular and developmental biology* **31**, 1327-1336.

Watt, A.J., Battle, M.A., Li, J. and Duncan, S.A., (2004). GATA4 is essential for formation of the proepicardium and regulates cardiogenesis. *Proceedings of the National Academy of Sciences of the United States of America* **101**, 12573-12578.

Yashiro, K., Shiratori, H. and Hamada, H., (2007). Haemodynamics determined by a genetic programme govern asymmetric development of the aortic arch. *Nature* **450**, 285-288.

Zhao, Z. and Rivkees, S.A., (2003). Rho-associated kinases play an essential role in cardiac morphogenesis and cardiomyocyte proliferation. *Developmental dynamics : an official publication of the American Association of Anatomists* **226**, 24-32.

Table 1. Number of embryos in somite groups per treatment (N= no injection, Ao= acrylamide only, AT= acrylamide and TEMED). .

	Treatment		
Somite Group	N	Ao	AT
<14	0	0	7
14-16	3	7	12
17-19	5	7	7
20-22	4	6	1
23-25	0	5	0

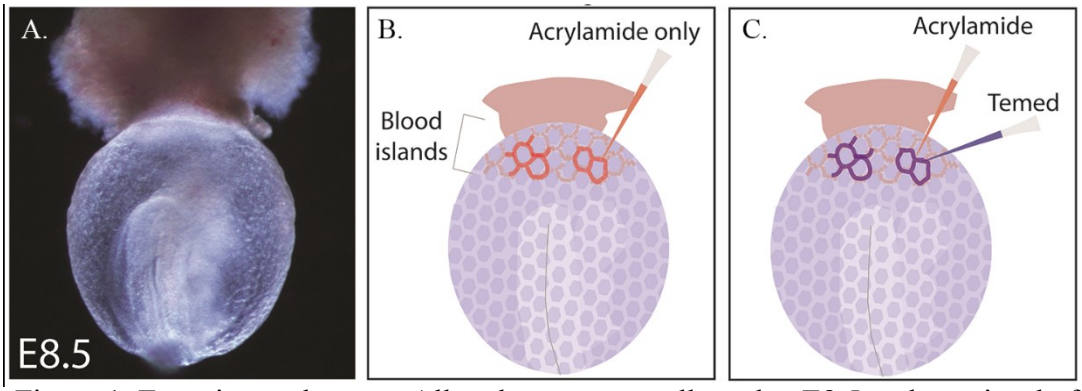

Figure 1. Experimental set up. All embryos were collected at E8.5 and consisted of the following groups: controls with no injections (N embryos) (A.), controls with only acrylamide injected into the blood islands (Ao embryos) (B.), and experimental embryos with both acrylamide and TEMED injected into the blood islands (AT embryos) (C.).

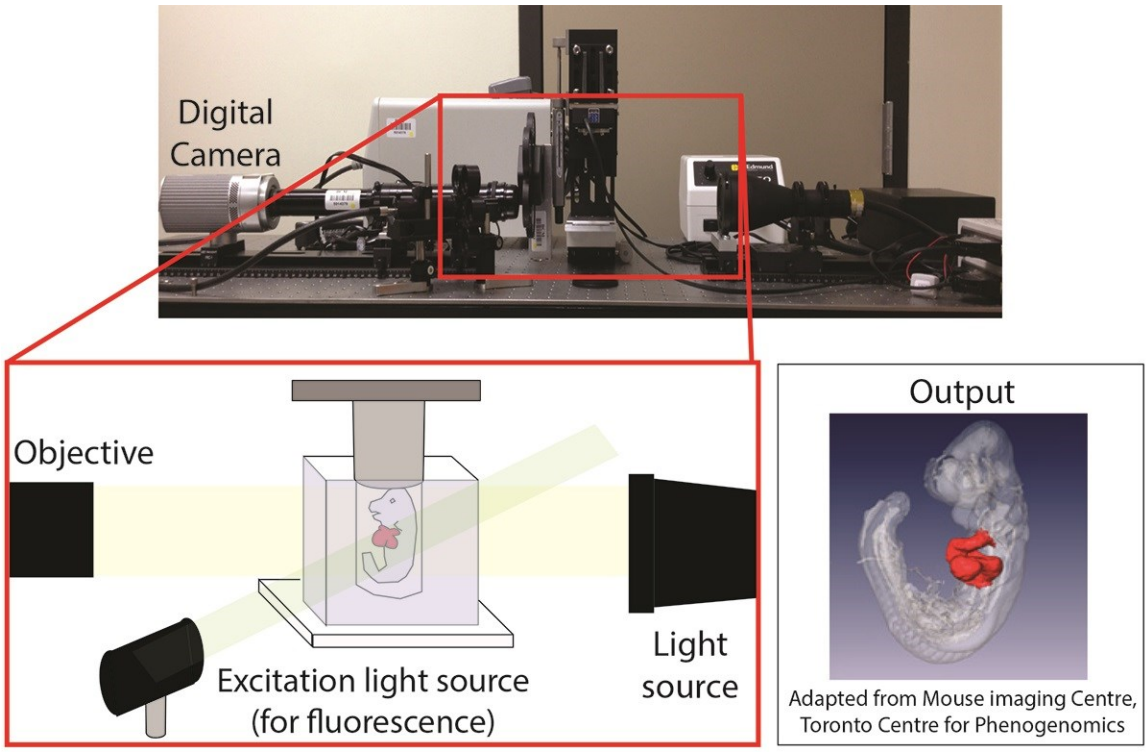

Figure 2. OPT set up**.** The OPT microscopy system consists of and excitation light source (as well as a white light source for autoflourescence), the specimen chamber with BABB, a motile and magnetic stage with a metal chuck with the specimen attached, and a camera to collect images directly onto a computer.

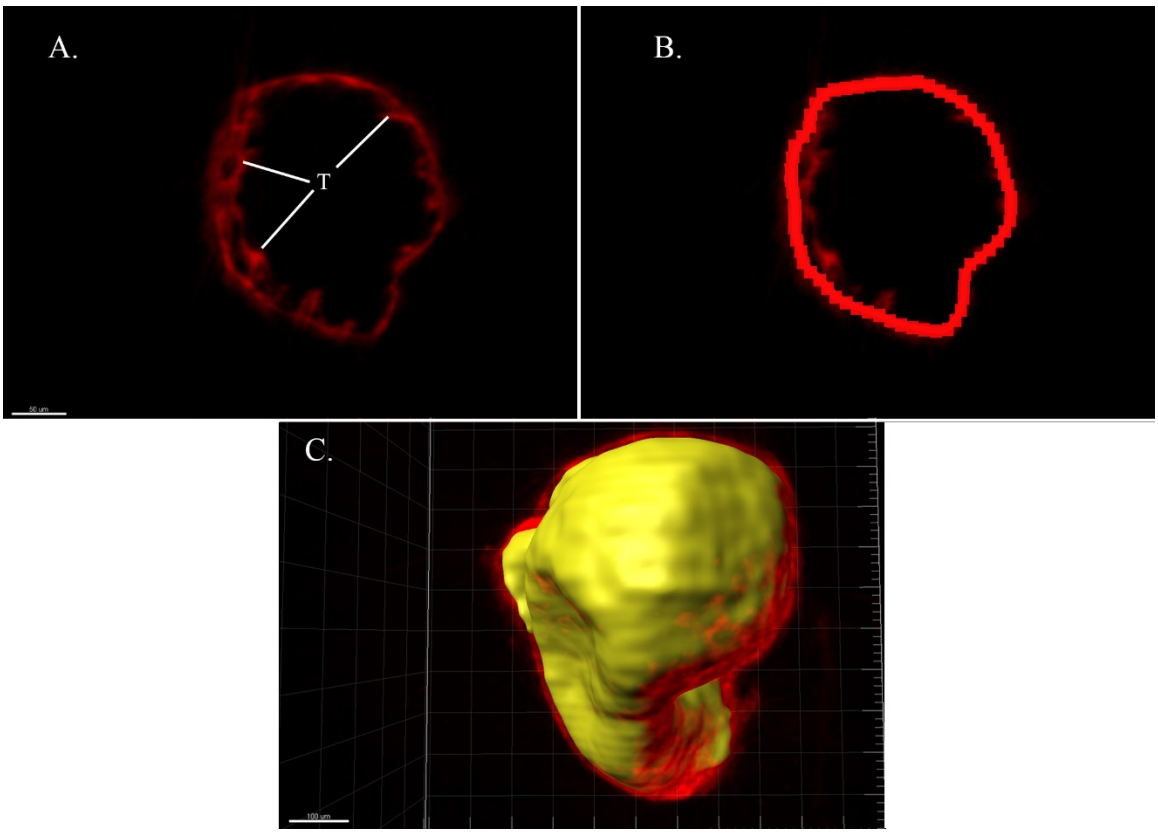

Figure 3. Volume data collection. Imaris was used to assess the volume of the hearts. This was accomplished by outlining the inner myocardium in multiple sections 10 um apart (A. & B.), and then combining these selections to create a volume (C.) that is then calculated by Imaris. (T=trabecula).

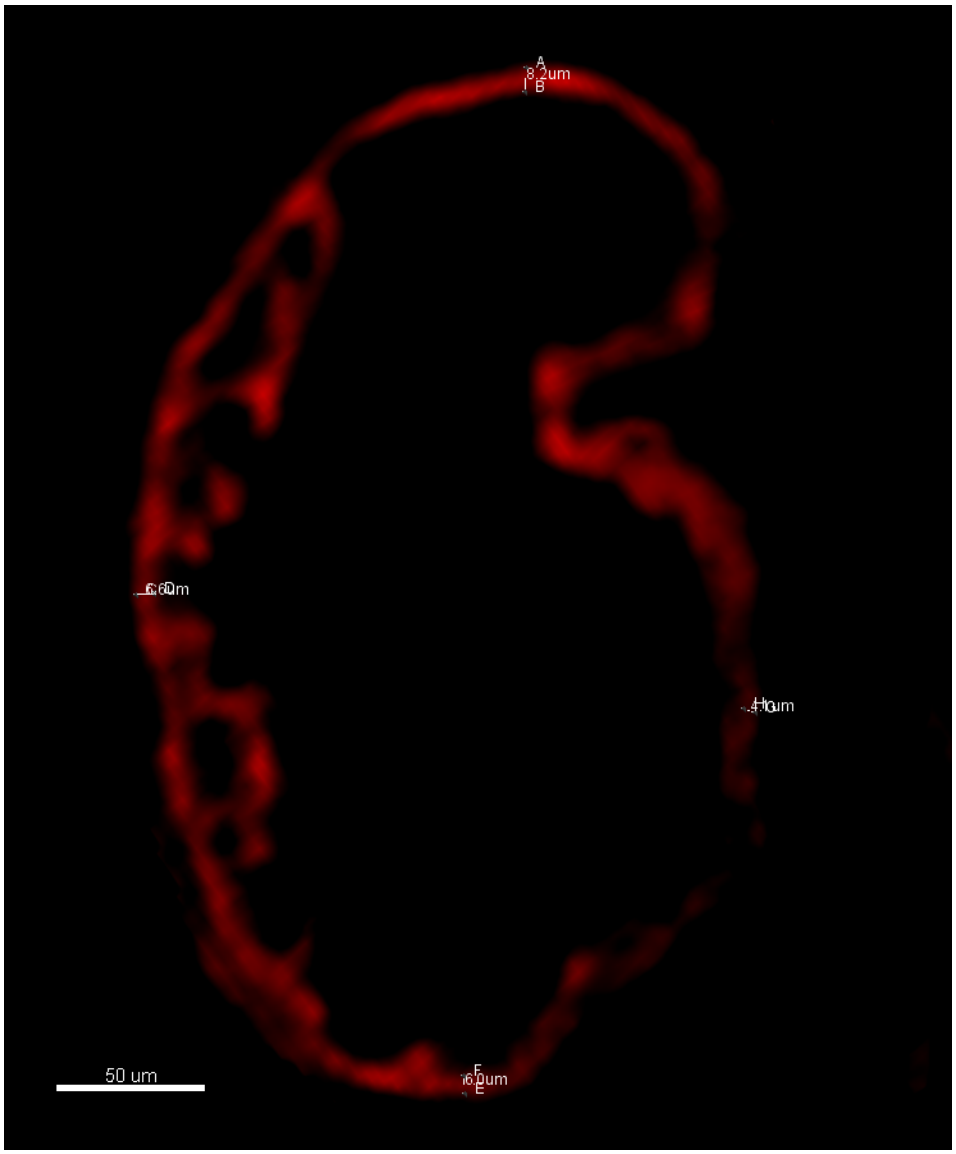

Figure 4. Myocardial thickness data collection**.** The myocardial thickness was measured in four places on five sections between the inflow to the outflow tracts.

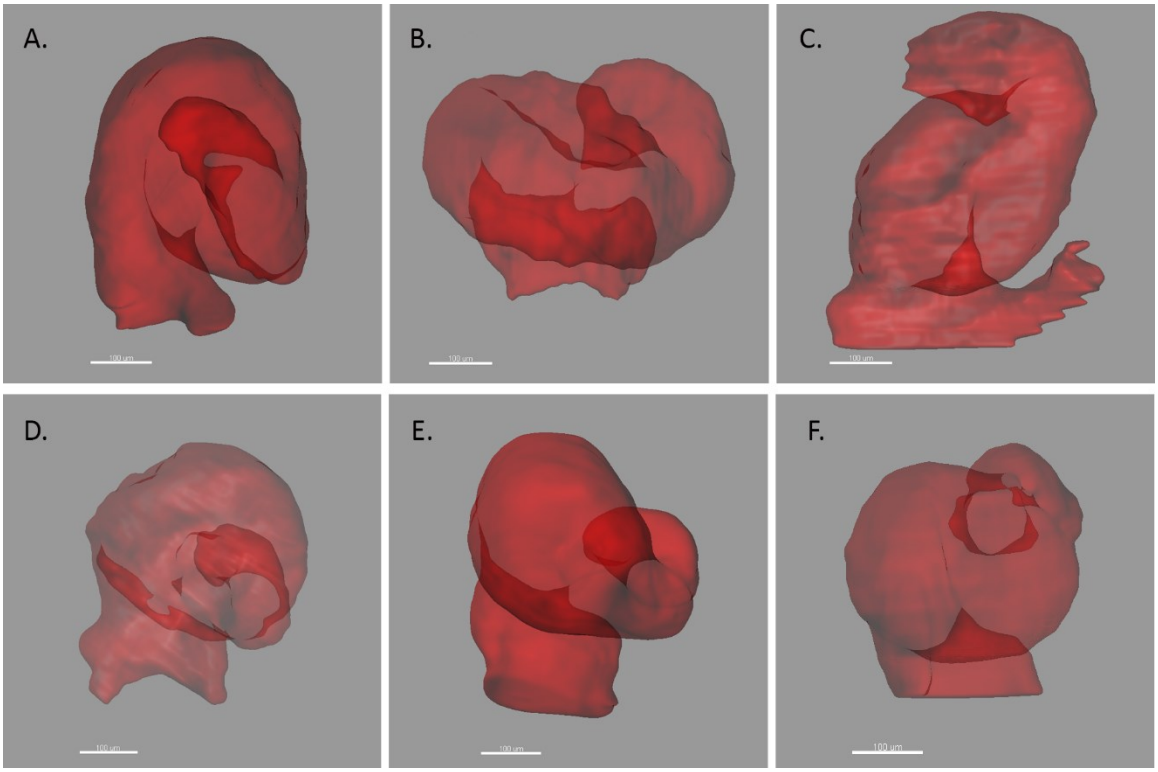

Figure 5. Representative images of volumes. Images of volumes used for the 14-16 somite range (N=A., Ao=B., AT=C.) and the 17-19 somite range (N=D., Ao=E., AT=F.). Scale bar 100 µm.

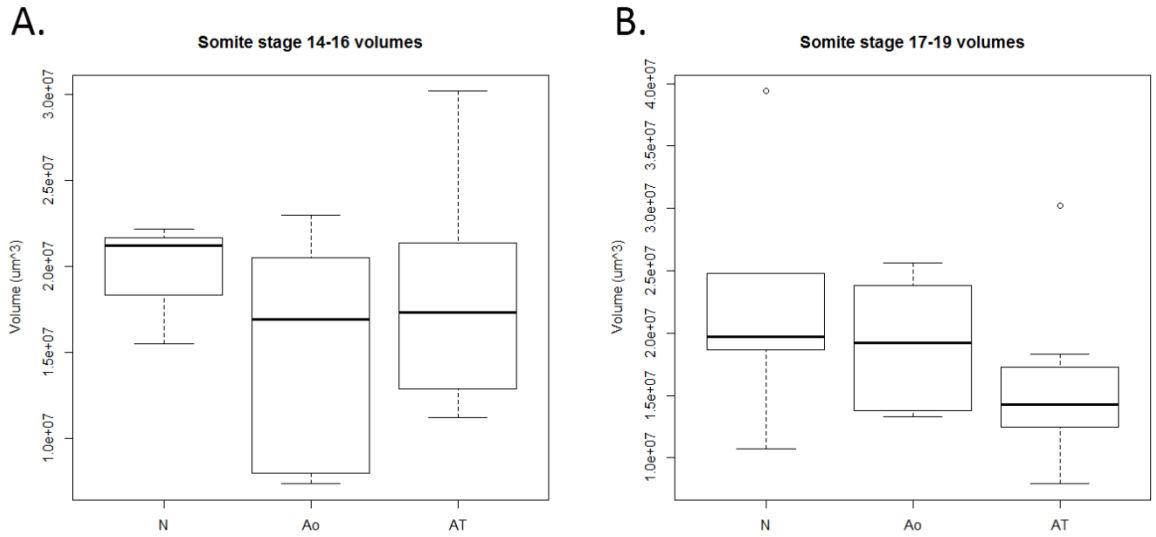

Figure 6. Decreased hemodynamic loading does not impact heart volume. Statistical analysis of heart volume at the 14-16 (A.) and 17-19 (B.) somite stages did not reveal a significant difference between the controls themselves (N to Ao), nor between the controls compared to the controls and experimental hearts (N to AT and Ao to AT $p>0.05$).

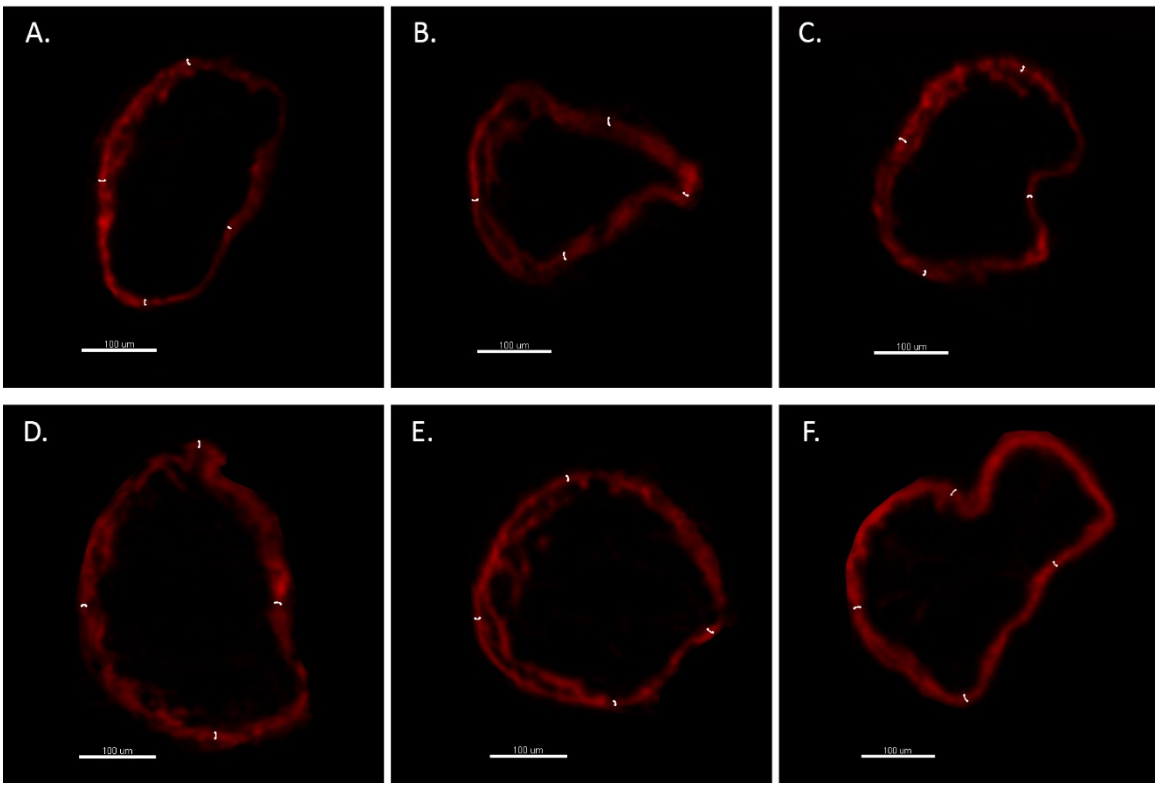

Figure 7. Representative images of myocardial thickness. Images of myocardial slices used for the 14-16 somite range (N=A., Ao=B., AT=C.) and the 17-19 somite range (N=D., Ao=E., AT=F.). Scale bar 100 µm.

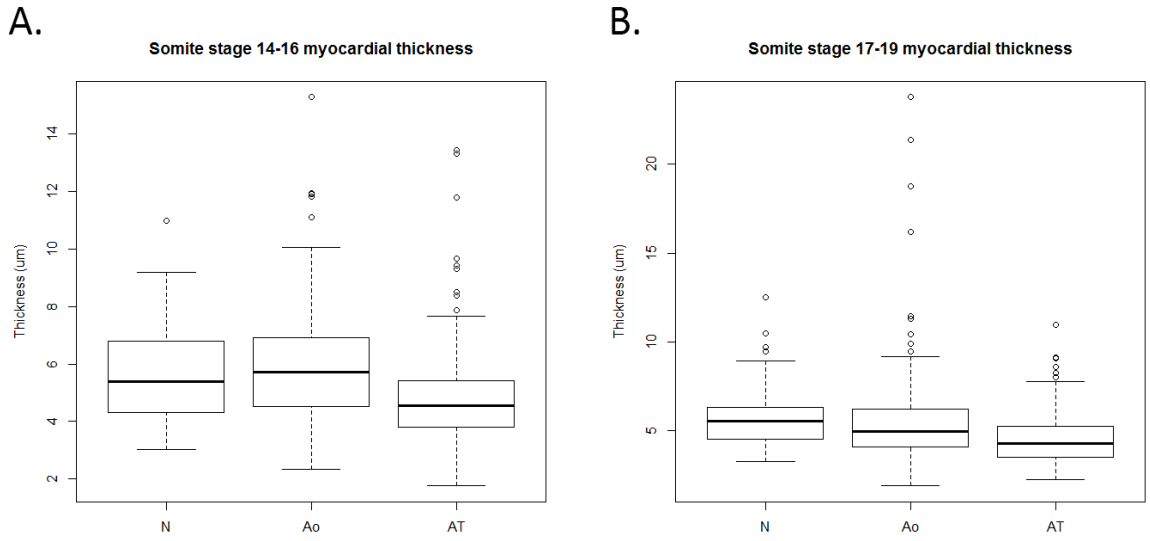

Figure 8. Myocardial thickness slightly decreases under low hemodynamic loading. Statistical analysis showed no difference in myocardial thickness at 14-16 (A.) and 17-19 (B.) somite stages between the controls (N and Ao). However, both somite stages showed a decrease in the myocardial thickness of AT embryos compares to the controls (N to AT and Ao to AT $p<0.05$).